11-18-2016

Magnon Spin Nernst Effect in Antiferromagnets

Vladimir Zyuzin
University of Nebraska-Lincoln, zyuzin.vova@gmail.com

Alexey Kovalev
University of Nebraska - Lncoln, alexey.kovalev@unl.edu

Magnon Spin Nernst Effect in Antiferromagnets

Vladimir A. Zyuzin and Alexey A. Kovalev
Department of Physics and Astronomy and Nebraska Center for Materials and Nanoscience, University of Nebraska, Lincoln, Nebraska 68588, USA
(Received 26 June 2016; revised manuscript received 26 October 2016; published 15 November 2016)

We predict that a temperature gradient can induce a magnon-mediated spin Hall response in an antiferromagnet with nontrivial magnon Berry curvature. We develop a linear response theory which gives a general condition for a Hall current to be well defined, even when the thermal Hall response is forbidden by symmetry. We apply our theory to a honeycomb lattice antiferromagnet and discuss a role of magnon edge states in a finite geometry.

DOI: 10.1103/PhysRevLett.117.217203

Understanding spin transport in nanostructures is a long-standing problem in the field of spintronics [1–3]. The discovery of the spin Hall effect [4–10] has been extremely important as it has led to many important developments in spintronics [11], such as the quantum spin Hall effect [12,13], the spin-orbit torque [14–16], and the spin Seebeck effect [17–19]. In the instrinsic spin Hall effect, the time reversal symmetry prohibits the transverse charge current but allows the transverse spin current originating from the nontrivial Berry curvature of electron bands [7,8]. The quantization of the intrinsic spin Hall effect can be characterized by the topological Chern number and is accompanied by the existence of topologically protected edges in the finite geometry [20]. On the other hand the quantum spin Hall effect can be characterized by the Z2 topological invariant [12,13].

The thermal Hall effect carried by magnons has been experimentally observed in collinear ferromagnets such as $Lu_2V_2O_7$, $Ho_2V_2O_7$, and $In_2Mn_2O_7$ with pyrochlore structure [21,22]. It has been understood that the Dzyaloshinskii-Moriya interaction (DMI) leads to the Berry curvature of magnon bands and to the transverse with respect to the external temperature gradient energy current [23–26]. The same effect has also been observed in kagome ferromagnet $Cu(1-3, bdc)$ [27]. The existence of magnon edge states and tunable topology of magnon bands has been discussed theoretically [24,25,28–31]. The spin Nernst effect (SNE) has been theoretically studied in Ref. [32] for a kagome lattice ferromagnet. Topological properties of honeycomb lattice ferromagnet were addressed in Refs. [33–35].

It has been recently realized that antiferromagnets are promising materials for spintronics applications [36]. In Refs. [37,38] the spin Seebeck effect has been studied in antiferromagnets. In Ref. [39] it has been shown that the Berry curvature can result in nonzero thermal Hall effect carried by magnons in magnets with dipolar interaction and in antiferromagnets. However, SNE in antiferromagnets has not been addressed as all of the studies of anomalous magnon-mediated spin transport in magnetic materials have so far been done in ferromagnetic systems.

In this Letter, we study SNE in antiferromagnets with Néel order. We first derive a general operator that has a well-defined current in a general antiferromagnet. We then develop a linear response theory for such a current using the Luttinger approach of the gravitational scalar potential [40,41]. It is shown that the response is driven by a modified Berry curvature of magnon bands. We then apply our findings to antiferromagnets with Néel order where a well-defined current corresponds to the spin density. Various realizations of antiferromagnets with honeycomb arrangement of magnetic atoms have been suggested recently [42–46]. We consider single- and bilayer honeycomb antiferromagnets with antiferromagnetic interlayer coupling where the nearest neighbor exchange interactions and the second nearest neighbor DMI are present (see Fig. 1). We show that both models possess the magnon edge states in the finite geometry and discuss their role for SNE. For a single layer, we observe an interplay between the Berry curvature due to the lattice topology and DMI and find that the Berry curvature is not of the monopole type, contrary to a ferromagnet on a honeycomb lattice [34,35]. We also find that SNE can be present in antiferromagnets that are invariant under (i) a global time reversal symmetry (e.g., Fig. 1, right) or under (ii) a combined operation of time reversal and inversion symmetries (e.g., Fig. 1, left) which prohibits the thermal Hall response derived in Ref. [39].

Current in antiferromagnet.—Here we assume a general model of antiferromagnet insulator with a magnetic unit cell having N sites. The Hamiltonian of such a system is of Heisenberg type with exchange interactions, DMI, anisotropies, and others. Assuming that we know the order of the system, we study the magnon excitations around that order. The Holstein-Primakoff transformation from spins to boson operators can be employed to study the magnons (see Ref. [47], for example). In this way, the boson operators $\nu_j(\mathbf{r})$ and $\nu_j^\dagger(\mathbf{r})$, with $j \in (1, N)$, correspond to the jth element of the magnetic unit cell. The operators satisfy commutation relationship $[\nu_i(\mathbf{r}), \nu_j^\dagger(\mathbf{r}')] = \delta_{ij}\delta_{\mathbf{r}\mathbf{r}'}$. We then proceed to write a general form of a Hamiltonian describing the magnons,

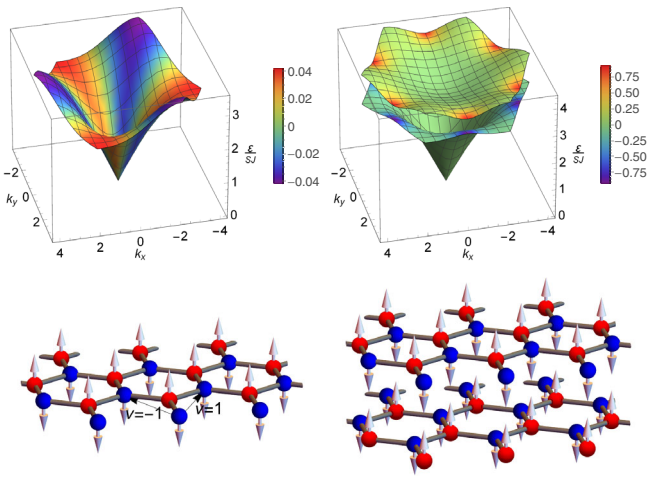

FIG. 1. Left: Magnon spectrum of a single layer antiferromagnet with DMI $D = 0.1J$ (black arrows correspond to ν sign convention of DMI), with schematics of the lattice and order in z direction in the bottom. Right: Magnon spectrum of antiferromagnet on a bilayer honeycomb lattice. Parameters are chosen to be $J' = J$ and $D = 0.1J$. In both cases the distribution of the Berry curvature over the Brillouin zone is plotted by the color distribution on top of the spectrum for one of the degenerate subbands.

$$H_0 = \frac{1}{2}\int d\mathbf{r}\Psi^\dagger(\mathbf{r})\hat{H}\Psi(\mathbf{r}). \tag{1}$$

Since this Hamiltonian describes magnons of an antiferromagnet, it will necessary contain pairing terms of boson operators. One must then extend the space of the Hamiltonian, such that the spinor $\Psi(\mathbf{r})$ is written as $\Psi(\mathbf{r}) = [\nu_1(\mathbf{r}), \ldots, \nu_N(\mathbf{r}), \nu_1^\dagger(\mathbf{r}), \ldots, \nu_N^\dagger(\mathbf{r})]^T$.

The Hamiltonian in $\mathbf{k}$ space can be diagonalized with a help of a paraunitry matrix $T_\mathbf{k}$, such that

$$T_\mathbf{k}^\dagger \hat{H}_\mathbf{k} T_\mathbf{k} = \varepsilon_\mathbf{k} = \begin{bmatrix} E_\mathbf{k} & 0 \\ 0 & E_{-\mathbf{k}} \end{bmatrix}, \tag{2}$$

where $E_\mathbf{k}$ is a $N \times N$ diagonal matrix of eigenvalues. Paraunitarity of the matrix $T_\mathbf{k}$ means that it has to satisfy a condition $T_\mathbf{k}^\dagger \sigma_3 T_\mathbf{k} = \sigma_3$.

We will be interested in responses of the system to external temperature gradient. To treat the temperature gradient we adopt the Luttinger method [40] and add gravitational potentials to the Hamiltonian as

$$H = \frac{1}{2}\int d\mathbf{r}\tilde{\Psi}^\dagger(\mathbf{r})\hat{H}\,\tilde{\Psi}(\mathbf{r}), \tag{3}$$

where $\tilde{\Psi}(\mathbf{r}) = [1 + (\mathbf{r}\boldsymbol{\nabla}\chi/2)]\Psi(\mathbf{r})$ with $\boldsymbol{\nabla}\chi$ being the temperature gradient with $\chi(\mathbf{r}) = -T(\mathbf{r})/T$.

Let us now introduce an arbitrary operator $\hat{O}$ acting in the Hilbert space of the studied system. The density of such an operator is $\mathcal{O}(\mathbf{r}) = \frac{1}{2}\Psi^\dagger(\mathbf{r})\hat{O}\Psi(\mathbf{r})$. Time evolution of the density is derived through a commutator with total Hamiltonian as, see Supplemental Material [48] for details, follows:

$$\begin{aligned}\frac{\partial\mathcal{O}(\mathbf{r})}{\partial t} &= i[H, \mathcal{O}(\mathbf{r})] \\ &= -\frac{1}{2}\boldsymbol{\nabla}\tilde{\Psi}^\dagger(\mathbf{r})(\hat{\mathbf{v}}\sigma_3\hat{O} + \hat{O}\sigma_3\hat{\mathbf{v}})\tilde{\Psi}(\mathbf{r}) \\ &\quad - i\frac{1}{2}\tilde{\Psi}^\dagger(\mathbf{r})(\hat{O}\sigma_3\hat{H} - \hat{H}\sigma_3\hat{O})\tilde{\Psi}(\mathbf{r}),\end{aligned} \tag{4}$$

where $\hat{\mathbf{v}} = i[\hat{H}, \mathbf{r}]$ is the velocity operator, and σ_3 is the third Pauli matrix operating in the extended space of the Hamiltonian (1). In deriving we assumed that the operator $\hat{O}$ commutes with the position operator. From Eq. (4) we observe that for the current of an operator $\hat{O}$ to be well defined, a

$$\hat{O}\sigma_3\hat{H} - \hat{H}\sigma_3\hat{O} = 0 \tag{5}$$

condition must be satisfied by the operator $\hat{O}$. Otherwise the quantity associated with the density $\mathcal{O}(\mathbf{r})$ will not be conserved in our system. Let us assume we have found such an operator that satisfies the condition (5), the current associated with this operator is then defined as

$$\mathbf{j}_\mathrm{O}(\mathbf{r}) = \tilde{\Psi}^\dagger(\mathbf{r})\hat{O}\sigma_3\hat{\mathbf{v}}\,\tilde{\Psi}(\mathbf{r}). \tag{6}$$

Let us now calculate the response of the $\hat{O}$-operator current to the temperature gradient. We will be working with the macroscopic currents, defined as $\mathbf{J}_\mathrm{O} = (1/V)\int d\mathbf{r}\mathbf{j}_\mathrm{O}(\mathbf{r})$, where V is the volume of the system. Note that the current consists of an unperturbed part $\mathbf{J}_\mathrm{O}^{[0]} = (1/V)\int d\mathbf{r}\Psi^\dagger(\mathbf{r})\hat{O}\sigma_3\mathbf{v}\Psi(\mathbf{r})$ and a perturbed by a temperature gradient $\mathbf{J}_\mathrm{O}^{[1]} = (1/2V)\int d\mathbf{r}\Psi^\dagger(\mathbf{r})\hat{O}\sigma_3(r_\beta\hat{\mathbf{v}} + \hat{\mathbf{v}}r_\beta)\Psi(\mathbf{r})\nabla_\beta\chi$ part. Both of them must be used to calculate linear response to the temperature gradient. The total current is

$$\mathbf{J}_\mathrm{O} = \langle\mathbf{J}_\mathrm{O}^{[0]}\rangle_\mathrm{ne} + \langle\mathbf{J}_\mathrm{O}^{[1]}\rangle_\mathrm{eq}. \tag{7}$$

The first term is evaluated with respect to nonequilibrium states and can be conveniently captured by the Kubo linear response formalism. Second current corresponds to orbital magnetization in the system and it is evaluated with respect to equilibrium state. To calculate the latter, we adopt the approach of Smrcka and Streda [49] and adopt derivations presented in Ref. [39]. It is important to note that the velocity written in the diagonal basis as $\tilde{v}_{\alpha\mathbf{k}} = T_\mathbf{k}^\dagger\hat{v}_\alpha T_\mathbf{k} = \partial_\alpha\varepsilon_\mathbf{k} + \mathcal{A}_{\alpha\mathbf{k}}\sigma_3\varepsilon_\mathbf{k} - \varepsilon_\mathbf{k}\sigma_3\mathcal{A}_{\alpha\mathbf{k}}$, is conveniently separated into diagonal and nondiagonal parts, where $\mathcal{A}_{\alpha\mathbf{k}} = T_\mathbf{k}^\dagger\sigma_3\partial_\alpha T_\mathbf{k}$. The latter is responsible for the transverse responses of the system. The details of the calculations for the current are given in Ref. [48]. Overall, the total current is derived to be

$$[\mathbf{J}_{\mathrm{O}}]_\alpha = \frac{1}{V}\sum_{\mathbf{k}n}[\bar{\Omega}^{[\mathrm{O}]}_{\alpha\beta}(\mathbf{k})]_{nn} c_1[(\sigma_3\varepsilon_{\mathbf{k}})_{nn}]\nabla_\beta\chi, \tag{8}$$

where $c_1(x) = \int_0^x d\eta\eta[dg(\eta)/d\eta]$, and $g(\eta) = (e^{\eta/T}-1)^{-1}$ is the Bose-Einstein distribution function. We defined an O-Berry curvature,

$$\bar{\Omega}^{[\mathrm{O}]}_{\alpha\beta}(\mathbf{k}) = i\bar{O}\partial_\alpha T^\dagger_{\mathbf{k}}\sigma_3\partial_\beta T_{\mathbf{k}} - (\alpha \leftrightarrow \beta), \tag{9}$$

a Berry curvature modified with an operator $\bar{O} = \sigma_3 T^\dagger_{\mathbf{k}}\hat{O}T_{\mathbf{k}}\sigma_3$. Because of the commutation relations (5), matrix $\bar{O}$ is diagonal in the band index. We show there is a sum rule $\sum_n[\bar{\Omega}^{[\mathrm{O}]}_{\alpha\beta}(\mathbf{k})]_{nn} = 0$ the O-Berry curvature satisfies. Expressions (8) and (9) together with (5) and (6) are the main results of this Letter.

Single layer honeycomb antiferromagnet.—We now apply our results to specific model of an antiferromagnet on honeycomb lattice. The lattice of the system is shown in Fig. 1. We define an exchange Hamiltonian

$$H = J\sum_{\langle ij\rangle}\mathbf{S}_i\mathbf{S}_j + D\sum_{\langle\langle ij\rangle\rangle}\nu_{ij}[\mathbf{S}_i\times\mathbf{S}_j]_z. \tag{10}$$

Here, $J>0$ is the nearest neighbor spin exchange, D is the strength of the second-nearest neighbor spin DMI, and ν_{ij} is a sign convention defined in Fig. 1.

Let us assume there is a Néel order in the direction perpendicular to the lattice plane, z direction. To study magnons of the model we perform a Holstein-Primakoff transformation from spins to boson operators, $S_{A+} = \sqrt{2S-a^\dagger a}a$, $S_{Az} = S - a^\dagger a$, and $S_{B+} = -\sqrt{2S-b^\dagger b}b^\dagger$, $S_{Bz} = -S + b^\dagger b$, and assume large S limit. As shown in the Supplemental Material [48], the Hamiltonian describing noninteracting magnons splits in to two blocks. The first block, call it I, is described by $\Psi_I = (a_{\mathbf{k}}, b^\dagger_{-\mathbf{k}})^T$ spinor. The Fourier image of the Hamiltonian of the first block is

$$H_{I\mathbf{k}} = JS\begin{bmatrix} 3+\Delta_{\mathbf{k}} & -\gamma_{\mathbf{k}} \\ -\gamma_{-\mathbf{k}} & 3-\Delta_{\mathbf{k}}\end{bmatrix}. \tag{11}$$

where we defined $\gamma_{\mathbf{k}} = 2e^{i(k_x/2\sqrt{3})}\cos(k_y/2) + e^{-i(k_x/\sqrt{3})}$, and $\Delta_{\mathbf{k}} = 2(D/J)[\sin(k_y) - 2\sin(k_y/2)\cos(\sqrt{3}k_x/2)]$ is the DMI, and we note $\Delta_{\mathbf{k}} = -\Delta_{-\mathbf{k}}$. Hamiltonian of the second block described by $\Psi_{II} = (b_{\mathbf{k}}, a^\dagger_{-\mathbf{k}})^{\mathrm{T}}$ spinor is obtained by $\gamma_{\mathbf{k}} \to \gamma_{-\mathbf{k}}$ in Eq. (11).

Let us define operator $\hat{O}$ acting in full, $\Psi_{\mathbf{k}} = (a_{\mathbf{k}}, b_{\mathbf{k}}, a^\dagger_{-\mathbf{k}}, b^\dagger_{-\mathbf{k}})^{\mathrm{T}}$, space as

$$\hat{O} = \begin{bmatrix}\hat{\tau}_3 & 0 \\ 0 & \hat{\tau}_3\end{bmatrix}, \tag{12}$$

where $\hat{\tau}_3$ is the third 2×2 Pauli matrix. The density of this operator written in real space, $\mathcal{O}(\mathbf{r}) = \frac{1}{2}\Psi^\dagger(\mathbf{r})\hat{O}\Psi(\mathbf{r}) = a^\dagger(\mathbf{r})a(\mathbf{r}) - b^\dagger(\mathbf{r})b(\mathbf{r})$, is the spin density. It can be shown that such an operator satisfies condition (5); thus, the spin density current associated with $\hat{O}$ is well defined. Let us now calculate the spin density current as a response to the temperature gradient. Expression for the response is given by Eq. (8); hence, we need to find eigenvalues and calculate the O-Berry curvature.

The spectrum of magnons for both blocks of the Hamiltonian is obtained to be

$$E_{\mathbf{k}} = JS(\Delta_{\mathbf{k}} + \sqrt{9-|\gamma_{\mathbf{k}}|^2}). \tag{13}$$

Paraunitary matrix $T_{I\mathbf{k}}$ that diagonalizes the Hamiltonian is readily constructed to be

$$T_{\mathrm{Ik}} = \begin{bmatrix}\cosh(\xi_{\mathbf{k}}/2)e^{i\chi_{\mathbf{k}}} & \sinh(\xi_{\mathbf{k}}/2) \\ \sinh(\xi_{\mathbf{k}}/2) & \cosh(\xi_{\mathbf{k}}/2)e^{-i\chi_{\mathbf{k}}}\end{bmatrix}, \tag{14}$$

where $\sinh(\xi_{\mathbf{k}}) = |\gamma_{\mathbf{k}}|/\sqrt{9-|\gamma_{\mathbf{k}}|^2}$, $\cosh(\xi_{\mathbf{k}}) = 3/\sqrt{9-|\gamma_{\mathbf{k}}|^2}$, and $\gamma_{\mathbf{k}} = |\gamma_{\mathbf{k}}|e^{i\chi_{\mathbf{k}}}$. One can show that the II block described by the $\Psi_{\mathrm{II}} = (b_{\mathbf{k}}, a^\dagger_{-\mathbf{k}})^T$ spinor has the paraunitary matrix T_{IIk} obtained from the T_{Ik} by setting $\chi_{\mathbf{k}} \to -\chi_{\mathbf{k}}$, and, hence, has the same O-Berry curvature (see Ref. [48] for more details). The spin density current can then be written as

$$[\mathbf{J}_{\mathrm{O}}]_\alpha = -\frac{1}{V}\sum_{\mathbf{k}} 2\Omega^{[\mathrm{O}]}_{\alpha\beta}(\mathbf{k})[c_1(E_{\mathbf{k}}) - c_1(E_{-\mathbf{k}})]\nabla_\beta\chi, \tag{15}$$

with the diagonal elements of the O-Berry curvature written as

$$\Omega^{[\mathrm{O}]}_{\alpha\beta}(\mathbf{k}) = -\frac{3}{2(9-|\gamma_{\mathbf{k}}|^2)^{3/2}} \times[(\partial_\alpha \mathrm{Re}\gamma_{\mathbf{k}})(\partial_\beta \mathrm{Im}\gamma_{\mathbf{k}}) - (\partial_\beta \mathrm{Re}\gamma_{\mathbf{k}})(\partial_\alpha \mathrm{Im}\gamma_{\mathbf{k}})]. \tag{16}$$

We observe that the current vanishes if the DMI is zero in the system, in which case $E_{\mathbf{k}} = E_{-\mathbf{k}}$. Note that the O-Berry curvature is independent of the DMI.

Recalling the definition of $\chi(\mathbf{r})$, we define SNE conductivity $\alpha^s_{\alpha\beta}$ as $[\mathbf{J}_{\mathrm{O}}]_\alpha = -\alpha^s_{\alpha\beta}\nabla_\beta T(\mathbf{r})$, and plot its dependence on the temperature; see Fig. 2. We now wish to extract analytic results in the limit of small DMI, $D<J$. There are two different symmetry points, namely, the $\mathbf{\Gamma}$ and $\mathbf{K}$, $\mathbf{K}'$ points in the Brillouin zone of magnons that the spin current gets major contributions from. Close to the $\mathbf{\Gamma} = (0,0)$ point the spectrum is ungapped and linear. We expand all functions close to the $\mathbf{\Gamma}$ point to obtain a low temperature $T<JS$ dependence of the current. See the Supplemental Material [48] for details.

$$[(\mathbf{J}_{\mathrm{O}})_x]_{\mathbf{\Gamma}} = \frac{5\zeta(5)}{9\sqrt{3}\pi V}\frac{D}{J}\left(\frac{T}{JS}\right)^4\nabla_y T(\mathbf{r}), \tag{17}$$

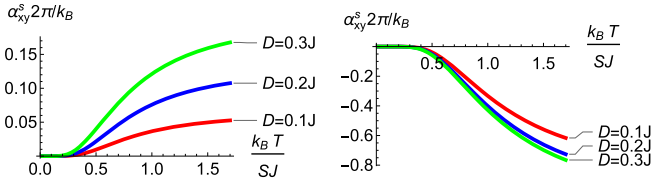

FIG. 2. Spin Nernst conductivity α^s_{xy}, defined after expression (15). Left: a single layer honeycomb antiferromagnet. Right: double layer honeycomb antiferromagnet. Plots are given for different values of DMI.

where an estimate of Riemann zeta function is $\zeta(5) \approx 1$. At the $\mathbf{K} = (0, -4\pi/3)$ and $\mathbf{K}' = (0, +4\pi/3)$ points, the Berry curvature has an absolute value maximum. An analytic estimate of the current contribution from these points at small temperatures $T < JS$, is obtained $[(\mathbf{J}_O)_x]_\mathbf{K} = (9\sqrt{3}\Lambda^2/8\pi V)(D/J)(JS/T)^2 e^{-(3JS/T)} \nabla_y T(\mathbf{r})$, where we introduced a high limit cutoff $\Lambda \sim 1$ for k, such that $\sum_\mathbf{k} = (\Lambda^2/4\pi)$. It is straightforward to show that $[(J_O)_x]_\Gamma \gg [(J_O)_x]_\mathbf{K}$ for small temperatures. Both contributions are of the same sign which always results in the same sign of SNE for this model irrespective of the temperature and the strength of the DMI.

The Chern number of the magnon band for the single layer honeycomb antiferromagnet is zero (see Fig. 1). As a result we do not observe any protected by the Chern number edge states in the finite strip geometry with a zigzag edge (see Fig. 3). Nevertheless, we observe an edge state analogous to the zero energy edge state in the fermionic model of graphene with a zigzag or bearded edge. The edge state connects the $\mathbf{K}$ and $\mathbf{K}'$ points, which have Berry curvatures different in sign. Such edge states do not contribute to the SNE in the finite geometry of a single layer honeycomb antiferromagnet.

Double layer honeycomb antiferromagnet.—In another model we consider an antiferromagnet on a double layer honeycomb lattice (see Fig. 1). We again assume a nearest neighbor antiferromagnetic exchange interaction, second-nearest neighbor DMI, same in both layers, and antiferromagnetic interaction between the layers denoted by J'. With

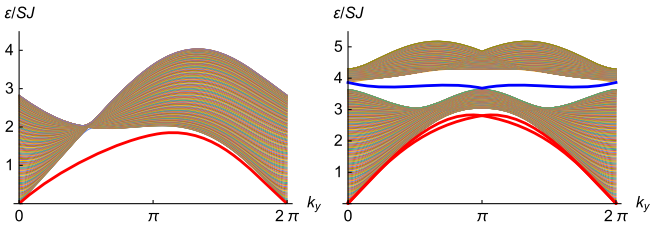

FIG. 3. Magnon spectrum of 80 atoms wide strip of honeycomb lattice antiferromagnet. Strip is in the x direction, while the y direction is assumed infinite. The edges of the system are of the zigzag type. Left: Single layer with DMI, $D = 0.2J$. Right: Double layer. Protected magnon edge states occur in the high energy band gap. Parameters are chosen to be $J' = 1.3J$ and $D = 0.2J$.

the Néel order being in the z direction, we follow the same steps as in the previous example and get a spectrum of spin waves

$$E^2_{\mathbf{k}\pm}/(SJ)^2 = \lambda^2 - |\gamma_\mathbf{k}|^2 + \Delta^2_\mathbf{k} - t^2 \pm 2\sqrt{\Delta^2_\mathbf{k}(\lambda^2 - |\gamma_\mathbf{k}|^2) + t^2|\gamma_\mathbf{k}|^2}; \quad (18)$$

here $\lambda = 3 + t$, where $t = J'/J$. The spectrum and the Berry curvature distribution is shown in Fig. 1. There we observe that the Berry curvature is of the monopole type located at the $\mathbf{M}$ points in the Brillouin zone in contrast to the magnon Haldane-Kane-Mele model [35].

For this model the Chern numbers of the upper and lower bands are $+1$ and -1, respectively, where the topological charge is $1/3$ per $\mathbf{M}$ point. The whole band now contributes in an additive way to SNE, which results in a much larger effect. Numerical calculations of the magnon SNE are shown in Fig. 2. To uncover the role of the edge states, we calculate the energy spectrum of a double-layer strip with a zigzag edge; see Fig. 3. The high-energy edge states here are due to DMI, in contrast to the single-layer model. These edge states are chiral and are protected by the finite Chern number due to the nontrivial topology of the bulk magnons. These edge states are also expected to contribute to SNE conductivity in the finite geometry [24]. The low-energy edge states are of the same nature as in a single layer honeycomb antiferromagnet and are not expected to contribute to SNE.

Absence of the thermal Hall effect.—The thermal Hall coefficient is given by an expression $\kappa_{xy} = -(1/2T)\sum_\mathbf{k} \sum_{n=1}^{2N} [\Omega_{xy}(\mathbf{k})]_{nn} c_2[(\sigma_3 \varepsilon_\mathbf{k})_{nn}]$, where we defined $c_2(x) = \int_0^x d\eta \eta^2 (dg/d\eta)$. We set $\hat{O} = \sigma_3$ in expression (9) to obtain the Berry curvature of the energy bands $\Omega_{xy}(\mathbf{k}) = i\sigma_3 \partial_x T^\dagger_\mathbf{k} \sigma_3 \partial_y T_\mathbf{k} - (x \leftrightarrow y)$. For an antiferromagnet on a single layer honeycomb lattice, the energy states are degenerate, corresponding to the two blocks, I and II, with opposite sign Berry curvatures. The two blocks correspond to two sublattices related either by inversion $\mathcal{I}$ or by time-reversal $\mathcal{T}$ transformations. On the other hand, the double layer antiferromagnet in Fig. 1 is invariant under the global time reversal symmetry if treated as a 2D system since $\mathcal{T}$ followed by interchange of honeycomb layers is a symmetry. Thus, the thermal Hall response considered in Ref. [39] vanishes for both models in Fig. 1.

Conclusions.—In this Letter we theoretically studied magnon mediated SNE in antiferromagnets. We gave a general condition for a current to be a well-defined quantity in an antiferromagnet, and then derived its response to an external temperature gradient. We showed that the transverse response of this current is defined by a modified Berry curvature. In antiferromagnets with Néel order, SNE can be driven by the Dzyaloshinskii-Moriya interaction and SNE is present even in systems with $\mathcal{TI}$ or global $\mathcal{T}$ symmetries. In both cases the thermal Hall effect is zero while SNE should change sign with the reversal of the Néel

vector in the former case but not in the latter case. We also identified the protected edge states with counterpropagating magnon modes, carrying spin but no energy.

We gratefully acknowledge useful discussions with K. Belashchenko. This work was supported by the DOE Early Career Award No. DE-SC0014189.

Note added—Recently, we became aware of a Letter [50] that discusses SNE in antiferromagnets. We believe the two Letters compliment each other.

[1] *Spin Physics in Semiconductors*, edited by M. I. Dyakonov (Springer-Verlag, Berlin, Heidelberg, 2008).
[2] I. Žutić, J. Fabian, and S. Das Sarma, Rev. Mod. Phys. **76**, 323 (2004).
[3] S. D. Bader and S. S. P. Parkin, Annu. Rev. Condens. Matter Phys. **1**, 71 (2010).
[4] M. I. Dyakonov and V. I. Perel, Phys. Lett. **35A**, 459 (1971).
[5] J. E. Hirsch, Phys. Rev. Lett. **83**, 1834 (1999).
[6] S. Zhang, Phys. Rev. Lett. **85**, 393 (2000).
[7] S. Murakami, N. Nagaosa, and S.-C. Zhang, Science **301**, 1348 (2003).
[8] J. Sinova, D. Culcer, Q. Niu, N. A. Sinitsyn, T. Jungwirth, and A. H. MacDonald, Phys. Rev. Lett. **92**, 126603 (2004).
[9] Y. K. Kato, R. C. Myers, A. C. Gossard, and D. D. Awschalom, Science **306**, 1910 (2004).
[10] S. O. Valenzuela and M. Tinkham, Nature (London) **442**, 176 (2006).
[11] J. Sinova, S. O. Valenzuela, J. Wunderlich, C. H. Back, and T. Jungwirth, Rev. Mod. Phys. **87**, 1213 (2015).
[12] C. L. Kane and E. J. Mele, Phys. Rev. Lett. **95** (2005), 146802.
[13] B. A. Bernevig, T. L. Hughes, and S.-C. Zhang, Science **314**, 1757 (2006).
[14] I. M. Miron, K. Garello, G. Gaudin, P.-J. Zermatten, M. V. Costache, S. Auffret, S. Bandiera, B. Rodmacq, A. Schuhl, and P. Gambardella, Nature (London) **476**, 189 (2011).
[15] L. Liu, O. J. Lee, T. J. Gudmundsen, D. C. Ralph, and R. A. Buhrman, Phys. Rev. Lett. **109**, 096602 (2012).
[16] L. Liu, C.-F. Pai, Y. Li, H. W. Tseng, D. C. Ralph, and R. A. Buhrman, Science **336**, 555 (2012).
[17] K.-I. Uchida, S. Takahashi, K. Harii, J. Ieda, W. Koshibae, K. Ando, S. Maekawa, and E. Saitoh, Nature (London) **455**, 778 (2008).
[18] K. Uchida, J. Xiao, H. Adachi, J. Ohe, S. Takahashi, J. Ieda, T. Ota, Y. Kajiwara, H. Umezawa, H. Kawai *et al.*, Nat. Mater. **9**, 894 (2010).
[19] C. M. Jaworski, J. Yang, S. Mack, D. D. Awschalom, J. P. Heremans, and R. C. Myers, Nat. Mater. **9**, 898 (2010).
[20] X.-L. Qi, Y.-S. Wu, and S.-C. Zhang, Phys. Rev. B **74**, 085308 (2006).
[21] Y. Onose, T. Ideue, H. Katsura, Y. Shiomi, N. Nagaosa, and Y. Tokura, Science **329**, 297 (2010).
[22] T. Ideue, Y. Onose, H. Katsura, Y. Shiomi, S. Ishiwata, N. Nagaosa, and Y. Tokura, Phys. Rev. B **85**, 134411 (2012).
[23] H. Katsura, N. Nagaosa, and P. A. Lee, Phys. Rev. Lett. **104**, 066403 (2010).
[24] R. Matsumoto and S. Murakami, Phys. Rev. Lett. **106**, 197202 (2011).
[25] L. Zhang, J. Ren, J.-S. Wang, and B. Li, Phys. Rev. B **87**, 144101 (2013).
[26] H. Lee, J. H. Han, and P. A. Lee, Phys. Rev. B **91**, 125413 (2015).
[27] M. Hirschberger, R. Chisnell, Y. S. Lee, and N. P. Ong, Phys. Rev. Lett. **115**, 106603 (2015).
[28] R. Shindou, R. Matsumoto, S. Murakami, and J.-i. Ohe, Phys. Rev. B **87**, 174427 (2013).
[29] R. Shindou, J.-i. Ohe, R. Matsumoto, S. Murakami, and E. Saitoh, Phys. Rev. B **87**, 174402 (2013).
[30] A. Mook, J. Henk, and I. Mertig, Phys. Rev. B **90**, 024412 (2014).
[31] A. Mook, J. Henk, and I. Mertig, Phys. Rev. B **89**, 134409 (2014).
[32] A. A. Kovalev and V. Zyuzin, Phys. Rev. B **93**, 161106 (2016).
[33] J. Fransson, A. M. Black-Schaffer, and A. V. Balatsky, Phys. Rev. B **94**, 075401 (2016).
[34] S. A. Owerre, J. Appl. Phys. **120**, 043903 (2016).
[35] S. K. Kim, H. Ochoa, R. Zarzuela, and Y. Tserkovnyak, arXiv:1603.04827 [Phys. Rev. Lett. (to be published)].
[36] T. Jungwirth, X. Marti, P. Wadley, and J. Wunderlich, Nat. Nanotechnol. **11**, 231 (2016).
[37] Y. Ohnuma, H. Adachi, E. Saitoh, and S. Maekawa, Phys. Rev. B **87**, 014423 (2013).
[38] S. M. Rezende, R. L. Rodríguez-Suárez, and A. Azevedo, Phys. Rev. B **93**, 014425 (2016).
[39] R. Matsumoto, R. Shindou, and S. Murakami, Phys. Rev. B **89**, 054420 (2014).
[40] J. M. Luttinger, Phys. Rev. **135**, A1505 (1964).
[41] G. Tatara, Phys. Rev. B **92**, 064405 (2015).
[42] A. A. Tsirlin, O. Janson, and H. Rosner, Phys. Rev. B **82**, 144416 (2010).
[43] X. Liu, T. Berlijn, W.-G. Yin, W. Ku, A. Tsvelik, Y.-J. Kim, H. Gretarsson, Y. Singh, P. Gegenwart, and J. P. Hill, Phys. Rev. B **83**, 220403 (2011).
[44] S. Lee, S. Choi, J. Kim, H. Sim, C. Won, S. Lee, S. A. Kim, N. Hur, and J.-G. Park, J. Phys. Condens. Matter **24**, 456004 (2012).
[45] Y. Singh, S. Manni, J. Reuther, T. Berlijn, R. Thomale, W. Ku, S. Trebst, and P. Gegenwart, Phys. Rev. Lett. **108**, 127203 (2012).
[46] S. K. Choi, R. Coldea, A. N. Kolmogorov, T. Lancaster, I. I. Mazin, S. J. Blundell, P. G. Radaelli, Y. Singh, P. Gegenwart, K. R. Choi *et al.*, Phys. Rev. Lett. **108**, 127204 (2012).
[47] A. Auerbach, *Interacting Electrons and Quantum Magnetism* (Springer, New York, 1994).
[48] See Supplemental Material at http://link.aps.org/supplemental/10.1103/PhysRevLett.117.217203 for details of calculations.
[49] L. Smrcka and P. Streda, J. Phys. C **10**, 2153 (1977).
[50] R. Cheng, S. Okamoto, and D. Xiao, preceding Letter, Phys. Rev. Lett. **117**, 217202 (2016).